

Growth rate influence on indium oxide thin films grown by an ultrasonic spray technique

R. Azizi^a, A. Attaf^a, H. Saidi^a, Y. Benkhetta^a, I. B. Kherkhachi^a, N. Attaf^b, M. Dahnoun^a and A. Bouhdjer^a

^a *Physics of thin films and applications laboratory, University of biskra, BP 145 RP, 07000 Biskra, Algeria.*

^b *Unité de Recherche "Sciences des Matériaux et Applications", Université Mentouri, Constantine, 25000, Algérie*

e-mail address of the corresponding author: ab_attaf@univ-biskra.dz

Received date: Feb. 20, 2019 ; accepted date: May 21, 2019

Abstract

Indium oxide (In_2O_3) thin films have been grown prosperously on glass substrates by an ultrasonic spray CVD process. The structural, morphological, optical and electrical studies of the films with controlled growth rate induced during elaboration by changing the solution flow rate from 20 to 60 mL/h. The X-ray diffraction (XRD) exhibit that the films are polycrystalline with centered cubic structure, whereas the predominant plane in the films change from (222) to (400) plane. The crystallite size of the films slightly increases with the increase of growth rate where it is varied between 26 and 32 nm. UV-Visible spectroscopy show that the average transmittance is about 80% in the visible region. The optical band gap decreases with an increase of the growth rate from 3.93 to 3.62 eV. Where the high value of band gap can be correlated with the preferential orientation of the (222) plane. The electrical resistivity decreases with the increase of the growth rate in the range of 20 - 5.5 ($10^2 \Omega \text{ Cm}$). From these results we can say that the indium oxide thin films have a promising properties which make them applicable in the photovoltaic field.

Keywords: Thin films, Indium oxide, Ultrasonic Spray, Growth rate, Electrical properties.

1. Introduction

Depending on the excellent optical and electrical properties for metal oxide semiconductor thin films. Numerous studies have been focused on them; the unique class of materials that depends on the metal oxides is Transparent Conducting Oxides (TCOs) which has both optical transparency and electrical conductivity. Among the most used TCOs materials, indium oxide (In_2O_3) is a versatile material with various wide applications and technological important. It is a TCO material of n-type semiconductor [1]. It has a wide band gap with a direct band gap around 3.5 - 3.8 eV [2] and an indirect band gap of about 2.6 eV [3]. It has a cubic structure with a lattice constant of $a = 10.117 \text{ \AA}$ and space group ($Ia\bar{3}$) [4]. High electrical conductivity and transparency of visible light, it is considerably used for photovoltaic devices, transparent windows, liquid crystal displays (LCD), solar cell, light emitting diode (LED), gas sensors and anti-reflecting coatings [5]. Most of undoped and doped In_2O_3 thin films are prepared by a variety of physical and chemical methods such as: spray pyrolysis [6], vacuum evaporation [7], magnetron sputtering [8], dc-sputtering [9], sol-gel [10], electron beam evaporation [11], reactive thermal evaporation [12] and pulsed laser ablation [13]. Among these deposition methods, spray pyrolysis is a preferred technique, it is versatile to fabricate thin films, not expensive, commercially viable, easy and simple to manipulate and applicable to large area.

The electrical conductivity of In_2O_3 films is due to transport of electrons. The high n-type conductivity detected in In_2O_3 films results from their anion paucity which is usually shown in the form of oxygen vacancies in the crystal network. However, when In_2O_3 film is perfectly stoichiometric, it can only be an ionic conductor. Such materials are not important as transparent conductors because of the high activation energy desired for ionic conductivity. In fact, the In_2O_3 films used for transparent conductors are barely perfectly stoichiometric. The previous explanation reveals a way to better the electrical properties of the In_2O_3 films, i.e. to prevent more oxygen incorporating into the films at the film growth process, but this is very complexed for the films deposited by ultrasonic spray process because the presence of O_2 molecular can not be avoided.

In order to prevent the incorporation of the oxygen molecular in the film network, we have increased in the value of the growth rate of these films [9] by increasing the quantities of the solution sprayed on the heated substrate. Furthermore, we have studied the influence of the growth rate on the films' textural, morphological, optical and electrical properties.

2. Experimental procedure

A 0.1 M of indium chloride InCl_3 (Merk, 99.9) is dissolved in methanol and sprayed onto heated glass substrates at 400 °C. Firstly, the substrates were cleaned with distilled water then dipped in acetone. Secondly, they're cleaned

with distilled water and were kept in methanol. Finally, the substrates were rinsed several times with distilled water then they left to dry in a hot air. In this work, we fixed the distance between spray nozzle and substrate at 5 cm. Furthermore, the deposition time was fixed during the spray process in atmospheric pressure at 2 min and we were changed only the growth rate which based on the change of the solution flow rate; that was controlled by (Syringe pump PHOENIX D-CP). Structural characterization is carried out with a D8 ADVANCE diffractometer using a Cu K_{α} radiation ($\lambda=1.5405 \text{ \AA}$). Morphological and topological surface studies are carried out using JOEL model JSM 6301F a scanning electron microscopy. Optical transmission spectra are recorded in the range of 200-800 nm using UV-VIS spectrophotometer. The electrical resistivity is determined using the four-point method.

3. Results and discussion

3.1. Growth rate

Fig.1 shows the growth rate variation as a function of solution flow rate and the films thickness change is given in the inset figure. The growth rate is estimated from the ratio of film thickness on the deposition time. As can be seen, the growth rate increases with the increase of solution's flow rate due to the increase of the volume solution sprayed on the substrate from 20 to 60 ml/h; however, it is interesting to note that the growth rate increases slightly at the beginning which indicates that the rate of horizontal growth in this case is faster than the perpendicular growth of the In_2O_3 films.

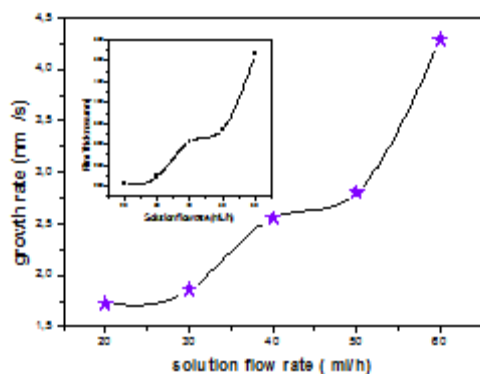
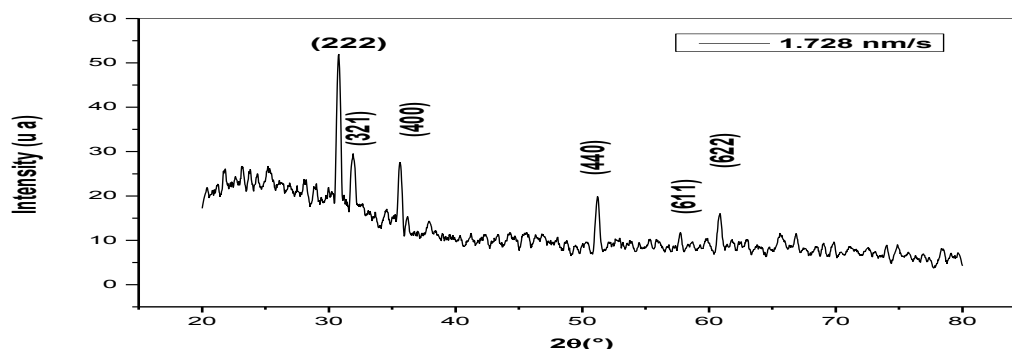


Figure 1. Growth rate as a function of solution flow rate and inset shows the film thickness dependence on

solution flow rate.

3.2. Structural properties.

Fig.2 shows the XRD patterns for In_2O_3 thin films grown at various growth rate. It is clear that the In_2O_3 thin films reveal polycrystalline structure with various orientated crystalline planes such as (222), (321), (400), (411), (156), (611), (440) and (622) which is agreed with the JCPDS card (n° 06-0416). However, there is a preferential growing competition between (222) and (400) planes, this indicates that the growth rate has important effect on the growth mechanism of the In_2O_3 films deposited by spray ultrasonic process. The influence of growth rate on the predominant growth orientation of the films evaluated by the peak intensity ratio $I(400)/I(222)$ (see figure 3). Fig.3 shows that the $I(400)/I(222)$ increases with rising in the growth rate. Thilakan and all [14] found that the preferred orientation changed from (222) to (400) with the augment of the growth rate. Also, they have proved that $I(400)/I(222)$ increases with the increasing of deposition time [15] or with the film thickness increase [16]. The values of the peak intensity ratio obtained in this study indicate that the films grown to a high growth rate possess a high degree of texturing along the [100] direction. Although, the high surface free energy in the bixbyite structure is found in (100) texture [17]. This is owing to the quantity of oxygen in the film network, whereas increasing the growth rate reduces the accumulation of the oxygen in the films; this means that it represses more oxygen into the films during the film growth process [17], which will permit the presence of the preferred growth of (400) grains. In general, the change of the oxygen concentration in the films influences in the intensity of the films orientations. Sundry studies revealed that the decrease of the oxygen concentration in the In_2O_3 films represses the intensity of the (222) orientation and motivates the (400) orientation of the In_2O_3 films [18,19,20]. According to the characteristic peaks that appeared in XRD patterns, we can confirm that the cubic bixbyite structure of the prepared films have a lattice parameter smaller than the reported value 10.118 \AA for pure indium oxide [21]. This indicates the compression of unit cell volume which in turn reveals the presence of stress in all the films. When growth rate increases, the lattice parameter was found to increase impending near the value of pure indium at high growth rate. The expected reason for this is the increasing of the oxygen vacancy in the films.



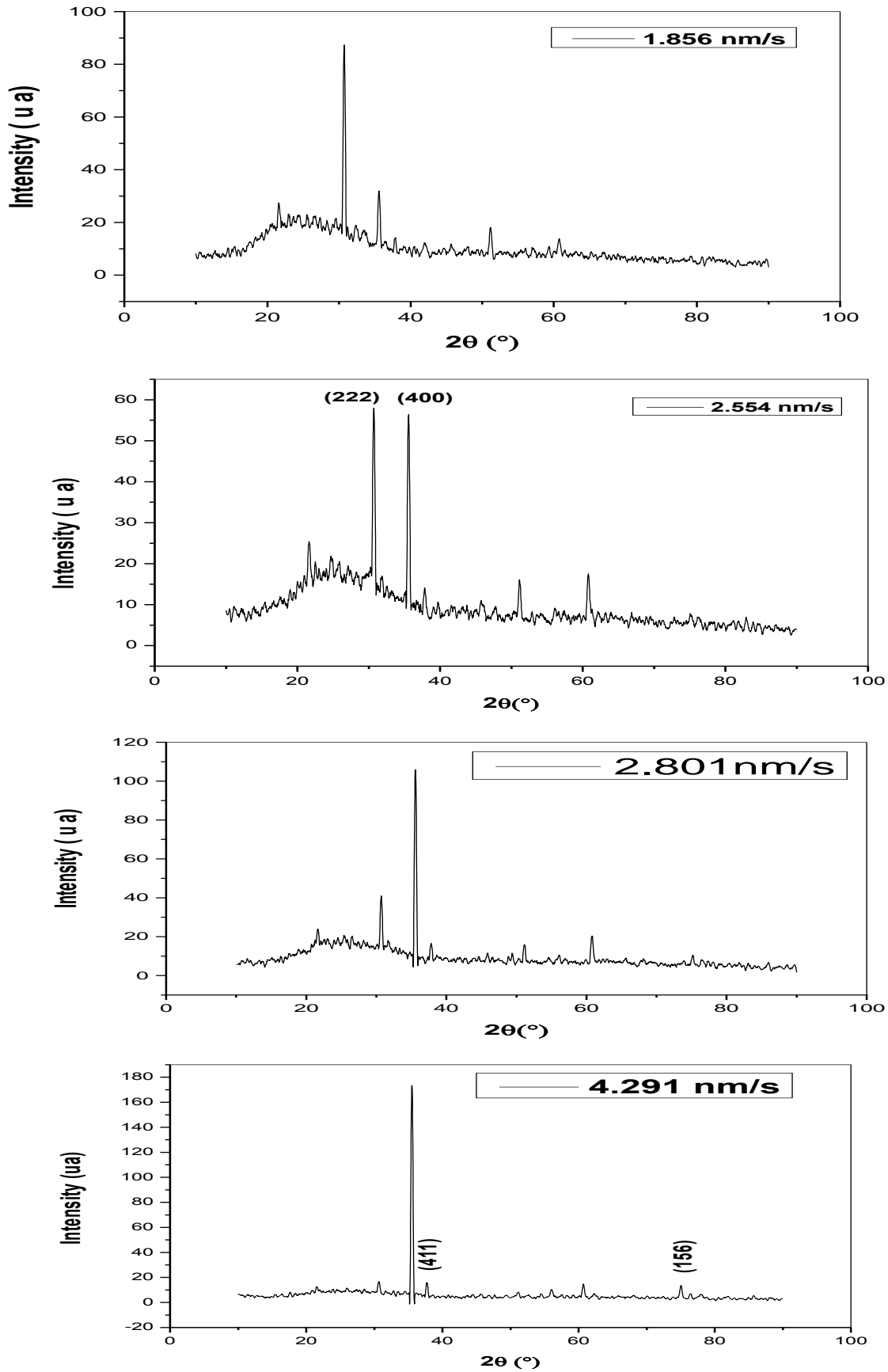


Figure 2. XRD pattern of In_2O_3 thin films deposited with different growth rates.

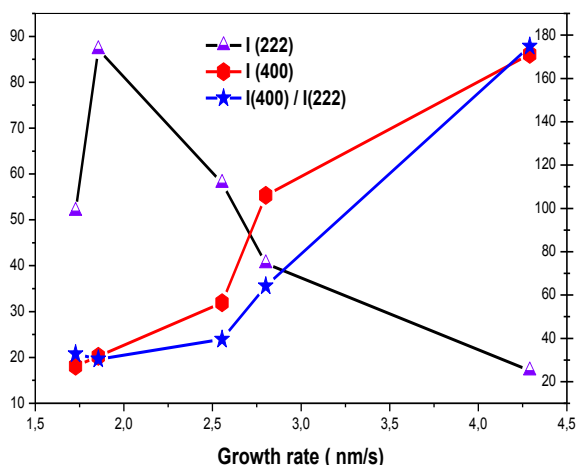


Figure 3. The Influence of the solution flow rate on the film growth rate.

The full width at half maximum (FWHM) of XRD line may be because of the crystallite size or the microstrain, whereas the crystallite size (D) of the In₂O₃ films is associated with (FWHM) by the classical formula of Scherrer given by [22]:

$$D = \frac{k\lambda}{\beta \cos \theta} \tag{1}$$

Where, the constant k is the shape factor (usually equal to 0.9), λ is the wavelength of X-ray. Table.1. reports the variations of the crystallite size. The crystallite size of the films was found in the range of 26- 32 nm. We have observed that the crystallite size is increased with the increasing of the growth rate which can be attributed to the amelioration of crystallinity. Also, when we increasing in the growth rate, the film formation process is fast yielding and the autographed amalgamation of droplets of solution above the substrate is due to the increased capacity of adatoms to move towards stable sites in the network. This means that best nucleation, larger crystallite size are formed from it[23]. However, it is clear that the increasing of crystallite size is very slight; the growth of In₂O₃ crystallite almost stops. This can be imputed to the fixed-increase of crystallite size with the rise of the film thickness up to 221 nm. G.Korotcenkov and all found the similar observation; when (D) is up to more than 30-35 nm, the growth of grains breaks off[16].

The mechanical strain in the films depends on two main influences which appear in metal oxide films [24]. The first one is the variation in the coefficients of thermal expansion of the materials of growing film and substrate. The second is the deflection of the growing film composition from stoichiometry which lead to the formation of the strain in

the lattice of films. The microstrain ε in the films is also correlated with (FWHM) by [25]:

$$\epsilon = \frac{\beta}{2 \tan \theta} \tag{2}$$

Where θ is the angle of Bragg and β is the full width at half maximum (FWHM).

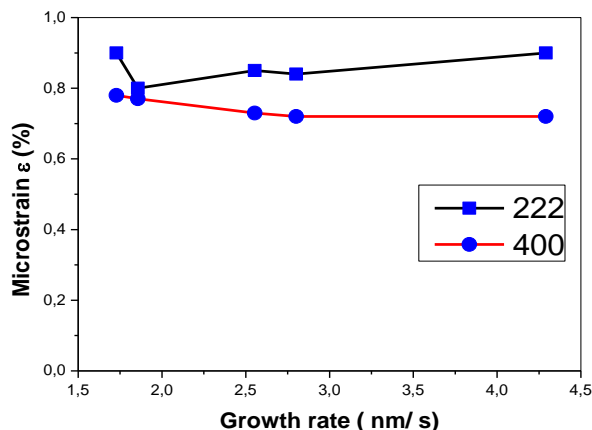


Figure 4. Microstrain ε as a function of growth rate

Fig.4 shows the microstrain of two delegate orientations as a function of growth rate. We have observed that the microstrain generally decreases with the increase of growth rate (film thickness), and we have noted that the microstrain of (400) orientation is always smaller than that of (222) orientation. Similar results shown that generally the microstrain rises with increasing in the distortion of lattice. This is physically reasonable because of the great oxygen interstitials which are incorporated in to the crystal lattice and the microstrain leading to larger of lattice distortion . In addition, it is observed that the big lattice distortion for the (222) orientation is compared with the other orientations[26].

Other effects influenced in the physical and mechanical properties of nanocrystalline materials which are dislocations: linear defects propagated in the plastic microstrain in the crystal lattice during their displacement. So, the value of the dislocation density (δ) which gives the defect numbers in the film was calculated from the crystallite size values D by the relationship[27]:

$$\delta = \frac{1}{D^2} \tag{3}$$

The dislocation density values were reported in Table 1. As we can see, the dislocation density decreases generally with the growth rate increasing in the two orientations. This may be due to the improvement of the films structure.

Table 1. Grain size, lattice parameter, optical band gap and disorder energy of In_2O_3 thin films as a function of the growth rate.

Growth rate (nm/s)	Solution flow rate (ml/h)	Lattice parameter $a=b=c$ (\AA)	Crystallite size (nm)		Band gap E_g (ev)	disorder energy E_{d0} (ev)	$\delta \cdot 10^{15}$ (lines/ m^2)	
			(222)	(400)			(222)	(400)
1.728	20	10.04	24.71	28.27	3.93	0.268	1.637	1.251
1.856	30	10.08	30.46	30.1	3.888	0.314	1.077	1.103
2.554	40	10.09	30.59	30.97	3.773	0.325	1.068	1.042
2.801	50	10.09	31.17	32.06	3.666	0.332	1.029	0.972
4.291	60	10.11	29,15	31.52	3.624	0.340	1.176	1.006

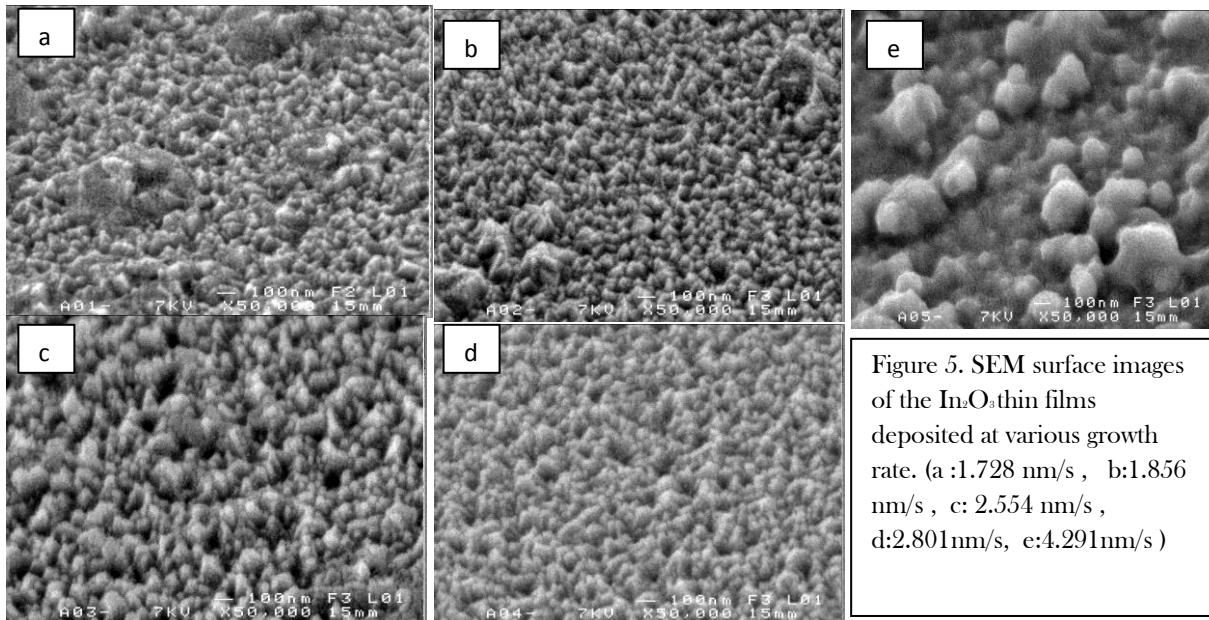


Figure 5. SEM surface images of the In_2O_3 thin films deposited at various growth rate. (a :1.728 nm/s , b:1.856 nm/s , c: 2.554 nm/s , d:2.801nm/s, e:4.291nm/s)

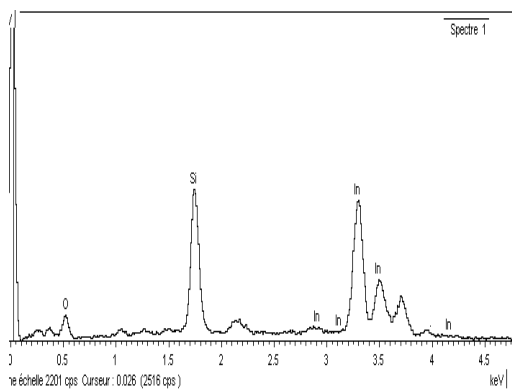


Figure 6. EDS analysis of the In_2O_3 thin film deposited at 2.554 nm/s.

3.3. Surface morphology

The surface morphology of In_2O_3 films are shown in Fig.5. We have observed that all the films have a homogeneous surface and relative roughness. Generally, the morphology does not change significantly except for the last film which is deposited at high growth rate (4.29 nm /s). It exhibit a dense inner structure with a lot of agglomerates up to the surface of the film. As we can see, the growth rate is lower than (4.29 nm /s), the shape of the grains in the thinner films is similar approximately to that reported for the thicker films with increasing in the growth rate, i.e., the grain size on top of the film does not change approximately. This result supports the XRD observations, but in the film deposited at 60 ml/h, we have observed that the agglomerates of very fine particles due to the high amount of solution.EDS analysis

of the In_2O_3 thin film deposited at growth rate (2.55 nm /s)show that the film iscomposited from O and In atoms in addition to Si which comes from the substrate(see figure 6).

3.4. Optical properties

The transmittance spectra in UV-visible region of the prepared In_2O_3 films are shown in Fig.7.

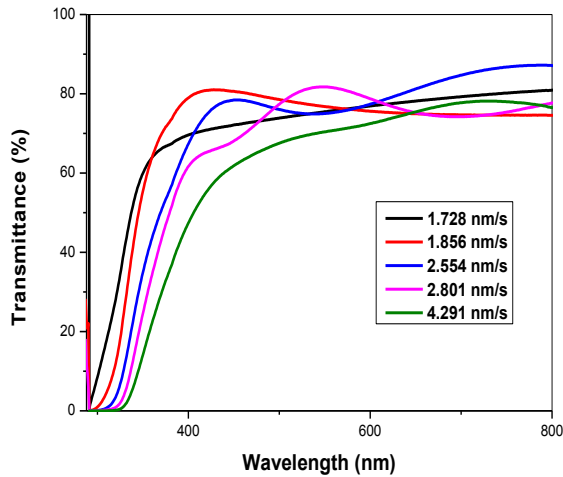


Figure 7. Optical transmittance spectra of In_2O_3 thin films as a function of growth rate.

We note that the growth rate affects the optical transmittance, whereas in the film deposited at low growth rate (1.728 nm/s), the transmittance is lower than the others except 4.291 nm/s although it has the smallest thickness. This result opposes with the previous different studies where they found that the lower thickness has height transmittance[28]. We can explain our result depending on the structure and the morphology of the films, whereas this sample has poor crystallinity and random orientation thickness as presented in Fig.5. This leads to more light scattering [29,30,31]. The energy loss due to light scattering and the microstrain is higher than other films; thus, it renders low optical transmittance. Furthermore, the optical transmittance in the rest of the films is higher than the last. Enhanced light transmitting due to continuous grain growth which is the best crystallinity films and of a reduced microstrain's effects, but in the high growth rate 4.291 nm/s, we have seen that the transmittance is smaller than all the films; it can be explained by the thickness of the film. It was found that there is an inversely relation between the transmittance and the thickness of the films. We have concluded that the films have structural homogeneity and the best crystallinity leading to less light scattering effects and higher transmittance. Moreover, with the increasing of the growth rate the absorption edge was moved to greater wavelengths suggesting the decrease of the energy band gap in the films.

The energy band gap was calculated using[32]:

$$(\alpha h\nu)^2 = A(h\nu - E_g) \tag{4}$$

Where, α is absorption coefficient, A is a constant, h is the Planck constant and E_g is the energy band gap of the semiconductor which was evaluated by proposing a direct transition between valence and conduction bands; by the extrapolation of the linear region to $(\alpha h\nu)^2 = 0$ [32].

Fig.8 shows the typical variation of the quantity $(\alpha h\nu)^2$ as a function of photon energy, inset shows the optical band gap energy as a function of growth rate. As we can see there is a decrease in the values of the optical band gap from 3.93 to 3.62 eV with an increase in the growth rate. It may be due to the increase of the lattice parameter. It is well-known that the various factors such as grain size, carrier concentration, presence of impurities, deviation from stoichiometry of the film and lattice constants change the E_g value[33]. Additionally, the film thickness increases resulting in a reduction of the band gap due to the localized states in the band structure which may amalgamate with the band edges given in the literature [34,35,14]. Furthermore, it is interesting to note that a high value of band gap can be correlated with the preferential orientation of the (222) plane. Similar behaviour in spray deposited In_2O_3 thin films where there is a high value of optical band gap which is obtained in the films deposited at low growth rate, whereas the peak (222) is the preferential orientation .

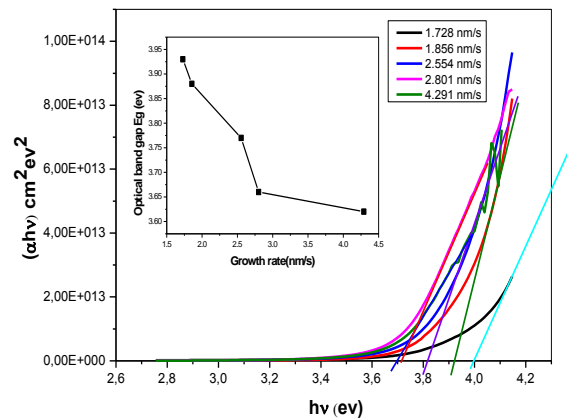


Figure 8. Typical variation of the quantity $(\alpha h\nu)^2$ as a function of photon energy, inset shows optical band gap energy with various growth rates.

The band gap is related to the oxidation of the components due to the oxygen concentration of the films in oxide semiconductors[35].

The formation of band tails due to the localized states which appear near the bands edges, and this leads to the disorder in film lattice showing in inset Fig. 9. In the low energies range, the photons are absorbed by these band tail states. In this range the absorption coefficient is given [36]:

$$\alpha = \alpha_0 \cdot \exp\left(-\frac{h\nu}{E_0}\right) \tag{5}$$

Where, α_0 is a constant and E_0 is the band tail commonly urbach tail or disorder energy, it is calculated from the slope of $\text{Ln}(\alpha)$ versus photon energy ($h\nu$). Fig .9 shows the disorder energy values variations with the growth rate. The

enhancement in the disorder energy values with the variation of growth rate which is changed due to the film growth mechanism, whereas at low growth rate the droplets is arrived slowly on surface substrate then they occupy a favorable site and organize themselves formally. However in high growth rate, the formation of the films are quickly leading to more disordered lattice. We also observe an inverse relation between the band gap and band tail as it shown in Fig.9. This is clear physically at the enhancement in the band tail that leads to the reduction of band gap presented in inset Fig .9.

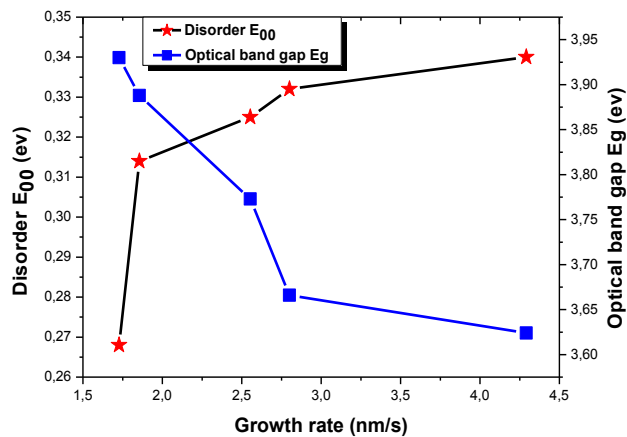


Figure 9. Variations of the optical band gap and disorder in thin films as a function of the growth rate. Inset figure is a schematic drawn of energy band diagram.

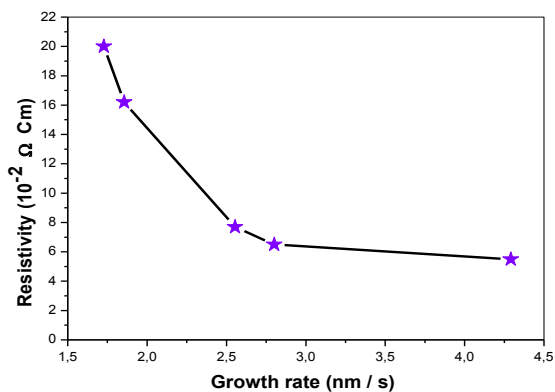


Figure 10. Electrical resistivity of In₂O₃ thin film with various growth rates.

3.5. Electrical properties

Fig.10 shows the electrical resistivity (ρ) as a function of the growth rate. The resistivity decreases with the increase in the growth rate. This is due to the quantity of oxygen in the films because as was noted already that the lower oxidation due to the deficiency of oxygen quantity in the films causes an increasing growth rate. It is common and physically reasonable that in oxygen deficient films, the carriers are resulted by the oxygen vacancies and the edge of conductivity band are formed by the defect of oxygen vacancies and/or in interstitials levels. Consequently, these impurity levels are responsible for low resistivity. Another

reason leads to the decrease of resistivity values that can be attributed to the improvement of the crystallization; however in our case, we believe that the improvements in the crystalline state don't affect the electrical properties because the growth of In₂O₃ crystallite almost stops as we said in The XRD results. On the other hand, it was observed that the resistivity of the films with (400) preferred plane is lower than the (222) preferred plane [35,14].

4. Conclusions

Indium oxide thin films are prepared by ultrasonic Spray technique onto glass substrates. An investigation of the influence of the growth rate on films properties is carried out. X-ray diffraction studies indicated that the nature of films is Polycrystalline, while the predominant plane in the film changes from normally occurring (222) plane to (400) plane. It is very sensitive to growth rate and the microstrain generally decreases with an increasing growth rate. As we have noted that the microstrain of (400) orientation is always smaller than that of (222) orientation and the dislocation density decreases with the growth rate increasing. These results indicate an improvement in the structural films. SEM images show that the films have homogeneous surface that is relatively rough. The morphology does not change significantly except for the last film with a change in the preferential growth orientation. As we found that the variation of the growth rate affected the optical properties of the films, whereas the films homogenous in structure and of the best crystallinity lead to less light scattering effects and a higher transmittance (about 80% in the visible region). The increase in growth rate leads to a decrease in the optical gap (from 3.93 to 3.62 eV), and the electrical resistivity ranges from 20 to 5.5 (10² Ω Cm).

References

- [1] S.T. Koida, H. Fujiwara, M. Kondo, *Solar Energy Materials & Solar Cells*. 93, (2009) 851-854
- [2] A. Walsh, J. L. Da Silva, S. H. Wei, C.Körber, A. Klein, L. F. J. Piper, ... & D. J. Payne, *Physical Review Letters*. 100, (2008) 167402
- [3] A. Raza, O.P. Agnihotri, B. K. Gupta, *Journal of Physics D: Applied Physics*. 10, (1977)1871.
- [4] M. Morezio. *Acta Crystallographica*. 20, (1966) 723
- [5] M.Girtan, H.Cachet, G. I. Rusua, *Thin Solid Films*. 427, (2003) 406-410.
- [6] J. C. Manificier; L.Szepessy, J. F. Bresse, M. Peroten, R. Stuck, *Mater. Res. Bull.* 14, (1979)109-119
- [7] K. R. Murali, V. Sambasivam, M. Jayachandran, M. J. Chockalingam, N. Rangarajan, V. K. Venkatesan, *Surf. Coat. Technol.* 35, (1988)297
- [8] W. G. Haines, R. H. Bube, *J. Appl. Phys.* 49, (1978) 304
- [9] Z. Qiaoa, R. Latzb, D. Mergela, *Thin Solid Films*. 466, (2004) 250
- [10] M. A. F. Mendoza, C. R. Perez, G. T. Delgado, J. M. Marín, O. Z. Angel, *Thin Solid Films*. 517, (2008) 681

- [11] S. M. Rozati, S. Mirzapour, M. G. Takwale, B. R. Marathe, V. G. Bhide, *Mater. Chem. Phys.* 36, (1994) 252
- [12] Chia-PuChu, Tsung-ShineKo, Yu-Cheng Chang, Tien-ChangLu, Hao-Chung Kuo, Shing Chung Wang, *Mater. Sci. Eng. B.* 147, (2008) 276
- [13] V. Marotta, S. Orlando, G. P. Parisi, A. Giardini, G. Perna, A. M. Santoro, V. Capozzi, *Appl. Surf. Sci.* 168, (2000) 141-145
- [14] P. Thilakan, J. Kumar, Studies on the preferred orientation changes and its influenced properties on IT0 thin films, *Vacuum.* 48, (1997) 463-466
- [15] A. Bouhdjer, A. Attaf, H. Saidi, H. Bendjedidi, Y. Benkhetta, I. Bouhaf, *Journal of Semiconductors.* 36, (2015) 8
- [16] G. Korotcenkov, V. Brinzari, A. Cerneavski, A. Cornet, J. Morante, A. Cabot, J. Arbiol, *Sens. Actuators B.* 84 (2002) 37-42
- [17] K. H. L. Zhang, A. Walsh, C. R. A. Catlow, V. K. Lazarov, R. G. Egdell, *Nano Letters.* 10, (2010) 3740-3746
- [18] E. Terzini, *Mater. Sci. Eng. B.* 77, (2000) 110
- [19] D. P. Pham, B. T. Phan, V. D. Hoang, H. T. Nguyen, T. K. H. Ta, S. Maenosono, C. V. Tran, *Thin Solid Films.* 570, (2014) 16-19
- [20] S. W. Sun, L. D. Wang, H. S. Kwok, *Thin Solid Films.* 360, (2000) 75
- [21] JCPDS Card n° 06-0416.
- [22] Y. Benkhetta, A. Attaf, H. Saidi, A. Bouhdjar, H. Benjdidi, I. B. Kherchachi, M. Nouadji, N. Lehraki, *Optik.* 127, (2016) 3005-3008
- [23] G. Korotcenkov, V. Brinzari, M. Ivanova, A. Cerneavski, J. Rodriguez, A. Cirera, A. Cornet, J. Morante, *Thin Solid Films.* 479, (2005) 38-51 (2005).
- [24] L. S. Palatnik, M. Y. Fuks, V. M. Kosevich, *Moscow, Science,* (1972) 320
- [25] L. I. Maissel, R. Glang (Eds.), *Handbook of Thin Film Technology*, McGraw-Hill Book Company, New York, USA, (1970).
- [26] Z. Qiao, D. Mergel, Comparison of radio-frequency and direct-current Magnetron sputtered thin $\text{In}_2\text{O}_3:\text{Sn}$ films, *Thin Solid Films.* 484, (2005) 146-153
- [27] I. B. Kherchachi, A. Attaf, H. Saidi, A. Bouhdjar, H. Bendjedidi, B. Youcef and R. Azizi, *Main Group Chemistry,* 15 (2016) 231-242
- [28] P. Prathap, N. Revathi, K. T. Ramakrishna Reddy, R. W. Miles, *Thin Solid Films.* 518, (2009) 1271-127.
- [29] P. Prathap, Y. P. V. Subbaiah, M. Devika, K. T. Ramakrishna Reddy, *Mater. Chem. Phys.* 100, (2006) 375.
- [30] P. Prathap, G. Gowri Devi, Y. P. V. Subbaiah, K. T. Ramakrishna Reddy, V. Ganesan, *Curr. Appl. Phys.* 8, (2008) 120
- [31] N. G. Pramod, S. N. Pandey, *Ceramics International.* 40, (2014) 3461-3468
- [32] A. Bouhdjer, A. Attaf, H. Saidi, Y. Benkhetta, M. S. Aida, I. Bouhaf, A. Rahil, *Optik.* 127, (2016) 6329-6333
- [33] N. G. Pramod, S. N. Pandey, *Ceramics International.* 41, (2015) 527-532
- [34] M. Higuchi, S. Uekusa, R. Nakano, K. Yokogawa, *J. Appl. Phys.* 74, (1993) 6710
- [35] P. Thilakan, J. Kumar, *Materials Science and Engineering B.* Vol. 55, (1998) 195-200
- [36] S. Benramache, B. Benhaoua, F. Chabane, A. Guettaf, *Optik.* 124, (2013) 3221-3224
- [37] Dong-Ju Kim, Bong-sueg Kim, Han-Ki Kim, *Thin Solid Films.* 517, (2013) 225-229